AMPHIBOLE OCCURRENCES IN METEORITES: NAKHLITE NORTHWEST AFRICA 13368 AND WINONAITE NORTHWEST AFRICA 13432.

P. K. Carpenter[1], A. J. Irving[2], and B. L. Jolliff[1], [1]Dept. of Earth and Planetary Sciences and McDonnell Center for the Space Sciences, Washington University, St. Louis, MO, USA (paulc@wustl.edu); [2]Dept. of Earth & Space Sciences, University of Washington, Seattle, WA, USA.

Introduction: We report the first analytical studies on recent meteorite finds Northwest Africa (NWA) 13368, a Martian nakhlite, and NWA 13432, a winonaite, which are of special interest as they both contain amphibole. Amphiboles are rare in meteorites and are present typically as micron-sized crystals making their recognition a challenge. Amphiboles identified in meteorites include anthophyllite, barroisite, ferri-magnesiohornblende, fluoro-edenite, fluoro-richterite, kaersutite, magnesio-arfvedsonite, magnesiohornblende, potassic-chloro-hastingsite, and winchite [1-5].

Analytical Methods: Bulk polished sections of the meteorites using backscattered-electron (BSE) imaging, X-ray mapping, and quantitative electron-probe analysis (EPMA) were analyzed using the JEOL JXA-8200 electron microprobe with Probe for EPMA operating system, at Washington University. Measurements using wavelength-dispersive spectrometry included the mean atomic number (MAN) background correction except for fluorine which used a polynomial background fit due to background curvature, and correction for interference from the Fe Lα X-ray line. Amphibole stoichiometric formulas and classification were made using the Excel sheet of Locock [6], and the amphibole analysis averages and formulas are listed in Table 1.

Nakhlite Northwest Africa 13368: NWA 13368 is a Martian nakhlite found in Mauritania in 2020 as a 1105 g stone [7]. The specimen is composed predominantly of euhedral, prismatic cumulus grains of augite (up to 1.3 mm) with thin, more ferroan rims plus subordinate (~4 vol.%) larger grains of olivine (up to 8 mm, with thin, more ferroan rims, enclosing unzoned augite) and sparse blocky grains of titanomagnetite (up to 0.7 mm) with a fine grained intercumulus assemblage of cruciform titanomagnetite, fayalite, hedenbergite, silica polymorph, pyrrhotite, and alkali feldspathic glass. "Iddingsitic" material occurs in thin veinlets within cumulus olivine grains. Fig. 1 shows BSE images of augite crystals, intercumulus relations, and an amphibole-bearing melt inclusion.

The mineral chemistry is as follows: augite cores $Fs_{23.0-24.7}Wo_{36.7-37.6}$, FeO/MnO = 28-31, Mg# 59-64%, with strongly zoned rims $Fs_{46.7-52.9}Wo_{44.2-33.8}$, FeO/MnO = 30-41, Mg# 14-16%; n = 346. Olivine cores $Fa_{61.5-62.7}$, FeO/MnO = 40-49, n = 30, and rims $Fa_{65-88.6}$, FeO/MnO = 37-51, n = 47. The intercumulus region contains hedenbergite ($Fs_{50.6-53.5}Wo_{41.2-40.6}$, FeO/MnO = 39-40, n = 2, fayalite ($Fa_{92.6-92.7}$, FeO/MnO = 36-37, n = 2, and an alkali feldspathic glass (approximately $Ab_{60.1}An_{19.4}Or_{20.4}$). Based on mineral chemistry, augite zoning profiles, and modal abundances, it is similar to MIL 03346 and paired specimens from Miller Range, Antarctica [8]. Melt inclusions within augite grains contain daughter crystals of potassic-chloro-hastingsite (KCH) with a high concentration of X-site Cl and elevated K and Fe (Table 1). Analyses of the amphibole from six melt in-

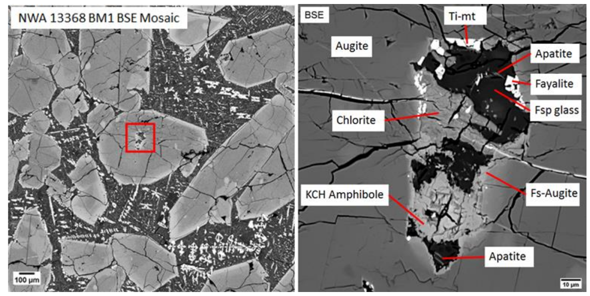

Figure 1. *Nakhlite NWA 13368, BSE images.*

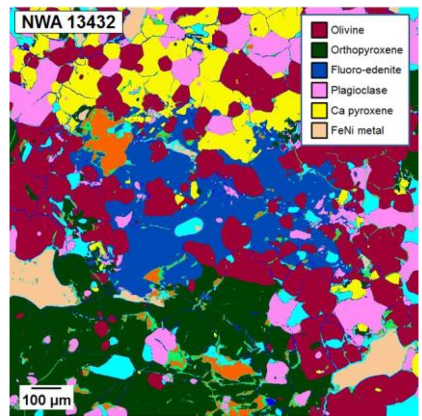

Figure 2. *Winonaite NWA 13432, cluster classification map.*

Table 1	Potassic-chloro-hastingsite				Fluoro-edenite			
	NWA 13368		MIL 03346		NWA 13432		HaH 193	
	n = 33	SD	n = 14	n = 1	n = 53	SD	A, n = 6	B, n = 17
SiO_2	35.67	1.33	37.48	35.60	50.10	0.71	49.7	50.03
TiO_2	0.44	0.48	0.38	0.24	1.00	0.14	0.63	1.08
Al_2O_3	10.69	1.35	8.62	10.40	6.61	0.26	5.89	5.88
Cr_2O_3	0.02	0.03			0.36	0.05	0.38	0.62
FeO	30.90	1.12	31.95	32.70	0.77	0.07	1.08	1.25
MnO	0.36	0.05	0.36	0.21	0.06	0.06	0.08	0.09
MgO	1.16	0.29	0.97	0.71	23.19	0.01	22.80	23.3
CaO	10.23	0.46	9.23	10.10	11.76	0.15	11.40	11.2
Na_2O	1.07	0.14	0.76	0.94	3.76	0.06	3.88	4.09
K_2O	3.08	0.19	2.52	3.27	0.57	0.06	0.45	0.48
P_2O_5	0.28	0.29	0.18	0.50	0.01	0.01		
F	nd		0.18		4.34	0.06	4.05	4.56
Cl	6.28	0.35	5.01	6.23	0.07	0.01	0.04	nd
O=F,Cl	1.42			1.41	1.85		1.71	1.92
Total	98.76		97.78	99.50	100.76		98.7	100.6
Note	nd = not detected		Sautter et al. 2006	McCubbin et al. 2009			Floss et al. 2007 Sections A and B	

NWA 13368 potassic-chloro-hastingsite, formula A B_2 M_5 T_8 O_{22} X_2 , A sum 0.939, B sum 2, M sum 5, T sum 8, X sum 2
$[K_{0.669} Na_{0.27}]$ $[Ca_{1.867} Na_{0.083} Mn_{0.05}]$ $[Fe^{2+}_{3.732} Fe^{3+}_{0.67} Mg_{0.295} Al_{0.242} Ti_{0.056} Cr_{0.003} Mn^{2+}_{0.002}]$ $[Si_{6.076} Al_{1.904} P_{0.02}]$ O_{22} $[Cl_{1.813} OH_{0.187}]$

NWA 13432 fluoro-edenite, formula A B_2 M_5 T_8 O_{22} X_2 , A sum 0.921, B sum 1.999, M sum 4.999, T sum 8, X sum 1.999
$[Na_{0.82} K_{0.101}]$ $[Ca_{1.747} Na_{0.191} Fe^{2+}_{0.041} Mg_{0.013} Mn_{0.007}]$ $[Mg_{4.781} Ti_{0.104} Fe^{3+}_{0.048} Cr_{0.039} Al_{0.027}]$ $[Si_{6.947} Al_{1.053}]$ O_{22} $[F_{1.903} OH_{0.08} Cl_{0.016}]$

Table 1. *EPMA analysis averages and calculated amphibole formula for NWA 13368 and NWA 13432, and comparison with amphibole from MIL 03346 and HaH 193.*

clusions have a uniform composition, and match analyses of KCH from inclusions in MIL 03346 [9,10]. The accommodation of Cl in the amphibole X-site is considered to be a function of Fe/Mg, tetrahedral Al, and A-site K based on natural and synthetic amphibole analysis, so that Cl preferentially occupies the X-site rather than OH or F [11,12]. Apatite from melt inclusions and intercumulus regions contains both F and Cl but the KCH has very low F, suggesting that the KCH partition coefficient for Cl is higher than observed for other bulk compositions [13], and that apatite records F content more effectively.

Melt inclusions exhibit an Fe-enrichment trend during crystallization of the inclusion. The Mg# is 60 in augite adjacent to the inclusion, 38 for transitional augite, 15 for ferroan augite on the interior inclusion wall, and 3-9 for KCH. The inclusions contain fayalite, Ti-magnetite, pyrrhotite, apatite and microcrystalline K-rich feldspathic glass. The modal abundance of the crystalline phases is variable, but they have a uniform composition. The enrichment within a melt inclusion is therefore similar to that shown in augite rim zoning profiles. The Cl content of inclusion glass is at least an order of magnitude higher than in the intercumulus glass and indicates high enrichment of Cl occurred during crystallization of the nakhlite melt.

Winonaite Northwest Africa 13432: NWA 13432 is a 4.46 kg winonaite found in 2020 [14]. It has a metamorphic texture with pervasive triple grain junctions, and is an aggregate of olivine, orthopyroxene, amphibole (as oikocrysts enclosing other mineral grains), sodic plagioclase, diopside and kamacite plus minor fluorapatite, graphite and schreibersite. A cluster classification map based on quantitative EPMA mapping shows the phase relations (Fig. 2). The mineral chemistry is as follows: olivine ($Fa_{3.0\text{-}3.3}$, FeO/MnO = 16-22, n = 5), orthopyroxene ($Fs_{3.5\text{-}3.8}Wo_{1.7\text{-}1.9}$, FeO/MnO = 12-14, n = 5), diopside ($Fs_{1.1\text{-}1.3}Wo_{44.8\text{-}45.8}$, FeO/MnO = 9-12, n = 3), and plagioclase ($An_{20.8}Ab_{76.5}Or_{2.6}$). The amphibole is classified as a fluoro-edenite (FE), which has a high concentration of F, with very low Cl (Table 1).

The FE exhibits a uniform composition throughout the specimen, and also is remarkably similar to FE from winonaite Hammadah al Hamra (HaH) 193 [2]. In both meteorites the FE is associated with diopside, olivine, orthopyroxene, and plagioclase. Floss et al. proposed the simplified reaction for replacement of clinopyroxene by FE as the reaction diopside + plagioclase + olivine = edenite:

$$MgCaSi_2O_6 + NaAlSi_3O_8 + 2\,Mg_2SiO_4 + CaF_2 = NaCa_2Mg_5AlSi_7O_{22}F_2$$

The component CaF_2 presumably represents either apatite or merrillite present as trace phases in winonaites. This reaction is substantiated by observation of FE closely associated with diopside, a minor component of the sample, and plagioclase, which has a lower modal abundance in regions where FE has formed. Winonaites have high Mg# and have equilibrated under highly reducing conditions, with Fe present as Fe^0 in metal and Fe^{2+} in silicates, but it is interesting to note Fe^{3+} is indicated in the amphibole formula recalculation.

Discussion: The amphibole halogen contents exemplify the association of Cl with Fe-rich, and F with Mg-rich bulk compositions. It is apparent that the amphibole composition exerts unit cell constraints on amphibole X-site occupancy, thus controlling the halogen species and concentration, though a feedback mechanism of Cl affecting Fe and K incorporation has been proposed [11, 15].

KCH from augite melt inclusions in nakhlite NWA 13368 contains an average of 6.28 wt% Cl and F is below detection. Micron-sized apatite in the augite melt inclusions contain 0.5 wt% F, 0.2-0.4 wt% Cl, and 0.1-0.3 calculated wt% OH, and thus has a higher F content compared to the KCH. Apatite from the intercumulus region contains 0.8 wt% F and 0.2 wt% Cl with no calculated OH. Inclusion glass contains 0.5 wt% Cl compared to 0.04 wt% in the intercumulus glass. The KCH-bearing augite melt inclusions thus appear to have recorded considerably higher Cl during the intermediate phase of augite crystallization.

FE from NWA 13432 contains 4.34 wt% F and 0.07 wt% Cl, and apatite contains 3.38 wt% F and 1.70 wt% Cl, which reflects the normal preferred incorporation of F vs. Cl in the amphibole X-site. Apatite is present in trace amount in NWA 13432, so it cannot be the source for F. We suggest that a F-bearing fluid phase has permeated portions of the winonaite body and leave a record in the amphibole halogen chemistry.

For the two studied meteorites, evaluation of amphibole mineralogy and halogen chemistry, and comparison with that of phosphate provide intriguing insight into both magmatic and metamorphic processes.

References: [1] Rubin A.E. and Chi, M. (2017) *Chemie der Erde, 77*, 325-385; [2] Floss C. et al. (2007) *Am. Min., 92*, 460-467; [3] McCanta M.C. et al. (2008) *Geochim. Cosmochim. Acta, 78*, 5757-5780; [4] Irving A.J. et al. (2017) *80th Meteorit. Soc. Mtg., Abstract #6383*; [5] Carpenter P. and Irving A.J. (2020) *Fall AGU Mtg., #V012-01*; [6] Locock, A.J., (2014) *Comp. Geosci. 62*, 1-11; [7] *Met. Bull. 109* (2020); [8] *Met. Bull. 89* (2005); [9] Sautter V. et al. (2006) *EPSL, 252*, 45-55; [10] McCubbin F.M. et al. (2009) *Geochim. Cosmochim. Acta, 73*, 4907-4917; [11] Henry, D.J. and Daigle N.M. (2018) *Am. Min., 103*, 55-68; [12] Jenkins, D.M. (2019) *Am. Min., 104*, 514-524; [13] Filiberto J. and Treiman A.H. (2009) *Geology, 37*, 1087-1090; [14] *Met. Bull. 109* (2020); [15] Geisting P. and Filiberto J. (2016) *MAPS, 51, n11*, 2127-2153.